Supplementary Information (SI) for Energy & Environmental Science.

Supporting Information

Guiding Vertical Growth and Improving Buried Interface of Pb-Sn Perovskite Film by 2D Perovskite Seeds for Efficient Narrow Bandgap Perovskite Solar Cells and Tandems

Jianxiong Yang,[1+] Zelin Wang,[1+] Xiaojia Zhao,[1+] Weiyin Gao,[1,3*] Gang Xing,[1] Xiaobo Wang,[1] Liangxu Wang,[1] Changbo Li,[1] Yuyi Wang,[1] Yumin Ren,[6] Wenjun Liu,[7] Fan Yang,[3] Jiaxiang Sun,[3] He Dong,[1] Lingfeng Chao,[2] Yipeng Zhou,[1] Yonghua Chen,[2] Zhongbin Wu,[1] Chenxin Ran,[1,4,5*] Wei Huang[1,2*]

[1]Frontiers Science Center for Flexible Electronics, Xi'an Institute of Flexible Electronics (IFE) and Northwestern Polytechnical University, Xi'an 710072, China.

[2]Key Laboratory of Flexible Electronics (KLOFE) & Institution of Advanced Materials (IAM), Nanjing Tech University (NanjingTech), Nanjing 211816, Jiangsu, P.R. China.

[3]Engineering Research Center of Smart Energy and Carbon Neutral in Oil & Gas Field Universities of Shaanxi Province, College of New Energy, Xi'an Shiyou University, Xi'an 710065, China.

[4]Research & Development Institute of Northwestern Polytechnical University in Shenzhen, Shenzhen 518063, China.

[5]Chongqing Innovation Center, Northwestern Polytechnical University, Chongqing 401135, China.

[6]School of Chemistry, Xi'an Jiaotong University, Xi'an, 710049, China.

[7]Frontier Institute of Science and Technology, State Key Laboratory of Electrical Insulation and Power Equipment, Xian Jiaotong University, Xian, 712046, China

+These authors contributed equally to this work.

+These authors contributed equally to this work.

E-mail: iamwygao@xsyu.edu.cn; iamcxran@nwpu.edu.cn; vc@nwpu.edu.cn

Experimental Section

Materials

Tin (II) iodide (SnI_2, 99.99%), tin (II) fluoride (SnF_2, 99.99%), lead thiocyanate ($Pb(SCN)_2$, 99.99%), ammonium thiocyanate (NH_4SCN, 99.99%), Chlorobenzene (CB, 99.8%), Dimethyl sulfoxide (DMSO, 99.97%)， glycine ethyl ester hydrochloride (GeeHCl, 99%), N-dimethylformamide (DMF, 99.8%), lead bromide ($PbBr_2$, 99.999%), Fluorophenethylamine iodide (F-PEAI, 99%), Anisole (99.7%) were purchased from Sigma-Aldrich. Lead iodide (PbI_2, 99.99%)，[4-(3,6dimethyl-9H-carbazol-9-yl)butyl]phosphonic acid (Me-4PACz, 99%), were purchased from TCI. Formamidinium iodide (FAI, 99.9%), methylammonium iodide (MAI, 99.9%), $PC_{60}BM$ were purchased from Advanced Election Technology. Toluene (TL, 99.7% AR), Ethyl Alcohol (ETOH, 99.7% AR), isopropanol (IPA, 99.7% AR) were purchased from Sinopharm Chemical Reagent Co., Ltd. Polyethylene glycol (PEG-1000) was purchased from Aladdin. PEDOT: PSS were purchased from Heraeus Clevios. BCP (99.5%) were purchased from Jinlin OLED Material Tech Co., Ltd.

Fabrication of Pb-Sn perovskite films and devices

<u>Preparation of Pb-Sn precursor solution.</u> 240.8 mg FAI, 95.6 mg MAI, 461.0 mg PbI_2, 372.5 mg SnI_2, 15.6 mg SnF_2, 3.4 mg GeeHCl, and 2.5 mg NH_4SCN were dissolved in 250 μL of DMSO and 750 μL of DMF, stirred 2 h at room temperature to prepare a 2.0 M $FA_{0.7}MA_{0.3}Pb_{0.5}Sn_{0.5}I_3$ precursors solution, and filtered through a 0.22 μm PTFE filter membrane for use.

<u>Preparation of $(F\text{-}PEA)_2PbICl_2SCN$ precursor solution.</u> 10.3 mg F-PEAI, 4.6mg PbI_2, 3.3 mg $Pb(SCN)_2$, 0.8 mg NH_4SCN,1 mg GEE were dissolved in a 1 mL mixed solution of DMSO and DMF (1:3 v/v) to make a 0.02 M precursor solution, after stirring 2 h at room temperature, which was filtered through a 0.22 μm PTFE filter membrane for use.

<u>Preparation of $EDAI_2$ precursor solution.</u> 0.5 mg $EDAI_2$ were dissolved in a 1 mL

mixed solution of IPA and toluene (1:1 v/v) to prepare a 0.5 mg/mL solution, stirred thoroughly at room temperature, and then filtered through a 0.22 μm PTFE filter membrane for use.

Deposition of substrates. The ITO glass was treated by UV-ozone for 15 min. For S-1 substrate, PEDOT: PSS was diluted with 1:6 water followed by sonicated for 20 minutes and filtered, and then spin-coated on ITO at 300 rpm for 3 seconds, 6000 rpm for 45 seconds, and annealed at 120 °C for 20 minutes. For S-2 substrate, F-PEA_2PbI_3SCN solution was spin-coated on S-1 at t 5000 rpm for 45 seconds, followed by annealing at 100 °C for 10 minutes. For S-3, 0.3 mg KSCN was added in 1 mL diluted PEDOT: PSS and sonicated for 20 minutes and filtered, and then spin-coated on ITO at 300 rpm for 3 seconds, 6000 rpm for 45 seconds, followed by the dropwise of PEG solution (0.55 mg/mL) for 28 seconds and annealed at 120 °C for 20 minutes. After that, F-PEA_2PbI_3SCN solution was spin-coated at t 5000 rpm for 45 seconds, followed by annealing at 100°C for 10 minutes.

Fabrication of Pb-Sn perovskite film. 50 μL Pb-Sn precursor solution was spin-coated on different substrates sequentially at 1000 rpm 10s and 5000 rpm for 45 s, and 350 μL of antisolvent (CB) was rapidly dropped at 20 s followed by annealed at 100 °C for 10 min. After cooling to room temperature, 30 μL $EDAI_2$ solution (0.5 mg/mL) was spin-coated at 5,000 rpm for 30 s and then annealed at 100 °C for 5 min.

Fabrication of device. After cooling the films to room temperature, PCBM (18 mg/mL in CB) was spin-coated at 1000 rpm 60s and 2000 rpm for 3 seconds. The device is completed by thermal evaporation of 6 nm BCP and 100 nm Ag electrode at the rate of 2 Å/s.

Fabrication of semi-transparent WBG Perovskite films and Device

Preparation of WBG Perovskite precursor solution. 165 mg FAI, 62.4 mg CsI, 221.4 mg PbI_2, 264.2 mg $PbBr_2$ were dissolved in a 1 mL mixed solution of DMF and DMSO (4:1 v/v), stirred 2 h to make a 1.2 M $Cs_{0.2}FA_{0.8}PbI_{1.8}Br_{1.2}$ perovskite precursors solution, which was filtered through a 0.22 μm PTFE filter membrane for use.

Fabrication of device. The cleaned and well-dried ITO glass was treated by UV-ozone for 20 min. Then, filtered NiO_x nanoparticle solution (10 mg/mL in water and IPA (3:1 v/v) was spin-coated on the ITO glass at 3000 rpm for 25 s followed by annealed at 100 °C for 10 min. The NiO_x/ITO substrate was transferred to an N_2 glove box, and 50 μl of Me-4PACz precursor solution (0.3 mg/mL in ethanol) was spin-coated at 3000 rpm for 25 s followed by annealed at 100 °C for 10 min. After cooling to room temperature, 50 μl WBG perovskite precursor solution was sequentially spin-coated at 5000 rpm for 32 s, and 250 μL of antisolvent anisole was rapidly dropped at 8 s followed by annealed at 100 °C for 15 min. After cooling to room temperature, 40 μL $PDAI_2$ precursor solution (0.5 mg/mL in IPA) was spin-coated at 3,000 rpm for 30 s and then annealed at 100 °C for 5 min. After cooling to room temperature, PCBM (18 mg/mL in CB) was spin-coated at 1000 rpm for 60 seconds and 2,000 rpm for 2 s. The device was fabricated by depositing a 20 nm layer of tin oxide (SnO_x) using atomic layer deposition (ALD) technology, and a 100 nm layer of indium tin oxide (ITO) was sputtered at a power of 50 W.

Precursor solution and film Characterization

The crystallization of the precursor solution on the substrates was observed by RTX series biological microscope and the static images were captured. Field Emission Scanning Electron Microscope (SEM) images were captured using the ZEISS Gemini SEM 300 (Carl Zeiss AG) at an accelerating voltage of 3 kV. Time-of-Flight Secondary Ion Mass Spectrometry (ToF-SIMS) of the perovskite film was performed and analyzed by Nanjing Demo Science Limited laboratory using a 3KV, 100 nA Ar ion cluster to sputter a 600×600 μm^2 sample surface with a cycle period of 10 s. In-situ UV-vis absorption spectra were obtained on a multi-spectrometer (DU-200, Shaanxi Puguang Weishi Co.Ltd.). X-ray diffraction (XRD) patterns were obtained using the Bruker D8 diffractometer with a maximum tube voltage of 60 kV and maximum tube current of 80 mA. Grazing Incidence Wide Angle X-Ray Scattering (GIWAXS) patterns were performed at the BL14B1 beamline of the Shanghai Synchrotron Radiation Facility (SSRF), using a wavelength of 1.24 Å, detector distance from sample of 359.45 mm, and grazing incidence angles of 0.1-0.6°. Atomic force microscopy (AFM) images were taken with the Cypher S Asylum Research Cypher S. (UV-Vis) were acquired using the Hitachi UH5700 absorption spectrophotometer. Kelvin Probe Force Microscopy (KPFM) images were taken using the Bruker Dimension Icon. UV-Visible spectrophotometer (UV-Vis) were acquired using the Hitachi UH5700 absorption spectrophotometer. Photoluminescence spectrum (PL) were obtained using the Edinburgh Instruments FLS1000 steady-state-transient fluorescence spectrometer. Ultraviolet Photoelectron Spectroscopy (UPS) were taken using the Shimadzu Kratos Axis Supra.

Device Characterization:

All the devices were tested in an N_2-filled glovebox using a Keithley 2400 source meter under a simulated AM1.5G spectrum and a solar simulator (EnliTech, Taiwan). The light intensity was calibrated to be 100 mW cm^{-2} using a NREL-certified monocrystalline Si diode (Newport 532 ISO1599). Data acquisition was carried out using a K-2400 source meter with a scanning range of -0.2 to 0.9 V (for WBG, the range was -0.2 to 1.35 V), with a scanning step of 0.02 V/step and a dwell time of 10 ms. The device performance parameters were calculated from the current-voltage curves of the photovoltaic device under 100 mW cm^{-2} with shadow masks area of 0.05 cm^2. Maximum power point (MPP) voltage was record for 180s under continuous standard AM 1.5G illumination. Dark current tests are conducted in the absence of external light stimulation, using a K-2400 digital source meter for recording and analysis. Electrochemical Impedance Spectroscopy (EIS) were recorded on Chenhua CH760 E. External Quantum Efficiency (EQE) was tested using the QTEST HIFINITY 5 external quantum efficiency measurement system under room temperature in air. Stability testing was performed at room temperature in a glove box filled with N_2.

For the Space Charge Limited Current (SCLC) test, the defect density of states is obtained from the equation:

$$N_{\text{trap}} = 2\varepsilon_0\varepsilon V_{\text{TFL}}/qL^2$$

where N_{trap} is the density of states of the defect, V_{TFL} is the initial bias voltage when the defect is filled, ε_0 is vacuum permittivity (8.82×10^{-14} F/cm^2), ε_r is relative permittivity of perovskite (~34), q is the amount of charge carried by a unit of positive charge (1.6 × 10^{-19} C), and L is the thickness of the light-absorbing layer of the perovskite film. The lattice strain ε of the films can be extracted from XRD patterns by fitting the slope in the Williamson-Hall plot:

$$\beta\cos\theta = 4\varepsilon\sin\theta + K\lambda/D_{size}$$

where, ε is the lattice strain, β is the half width of the characteristic peak of XRD, θ is the Bragg angle in radians, λ is the X-ray incident wavelength, K is the sharp factor, D_{size} is crystallite size.

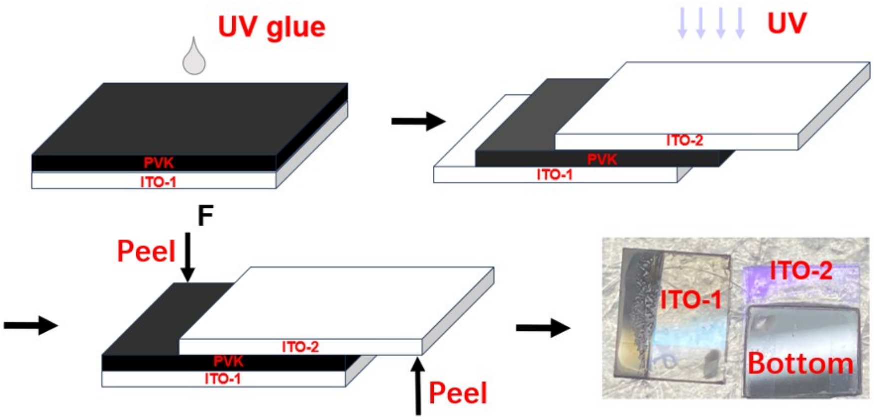

Figure S1. Schematic diagram of the peeling process of Pb-Sn film.

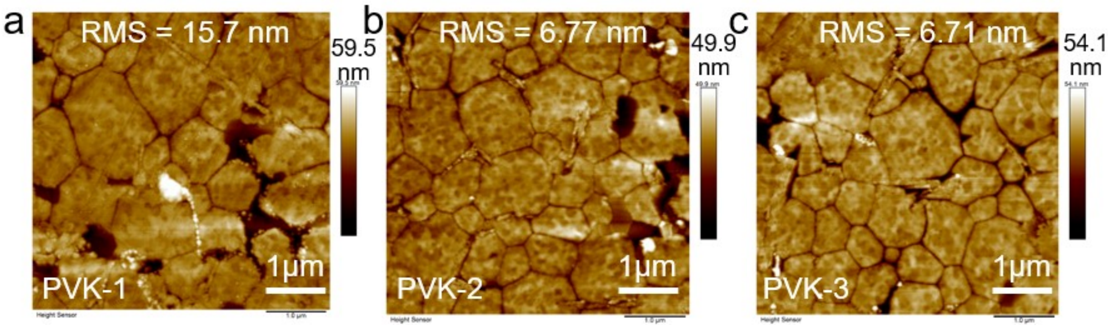

Figure S2. AFM of bottom surface of (a) PVK-1, (b) PVK -2 and (c) PVK -3.

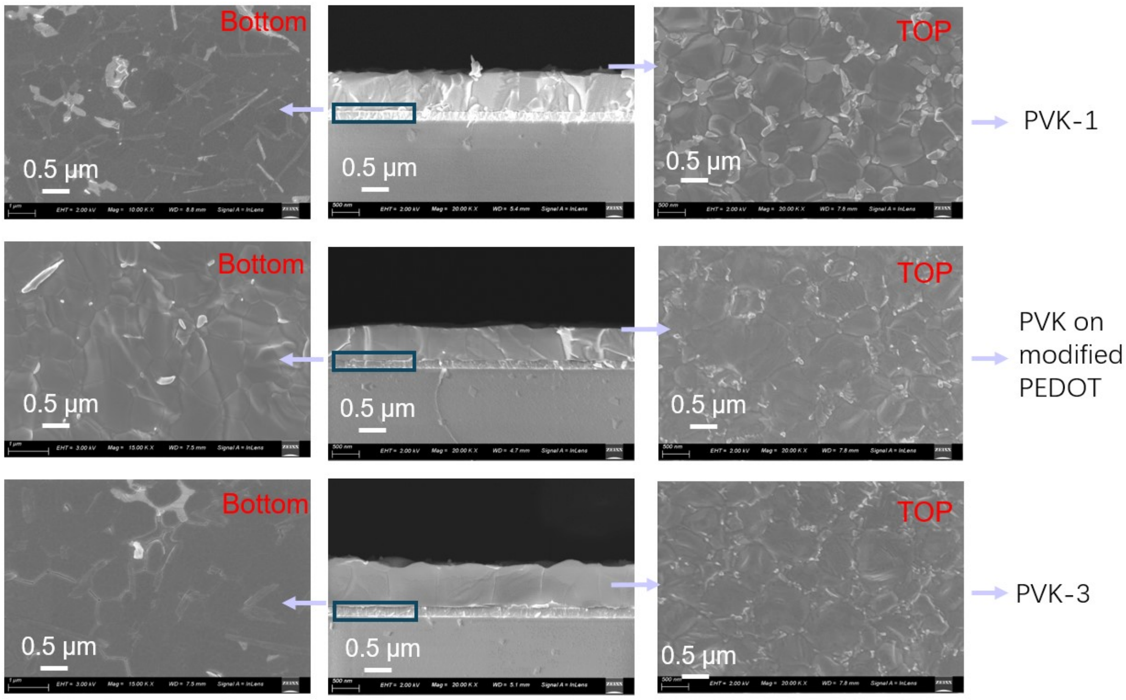

Figure S3. SEM images of PVK deposit on modified PEDOT: PSS, and PVK-1 and PVK-3 are for comparation.

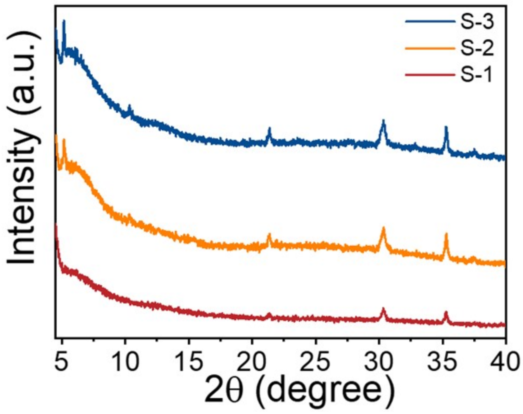

Figure S4. XRD pattern of different substrates, showing typical 2D perovskite peaks in S-2 and S-3 substrates.

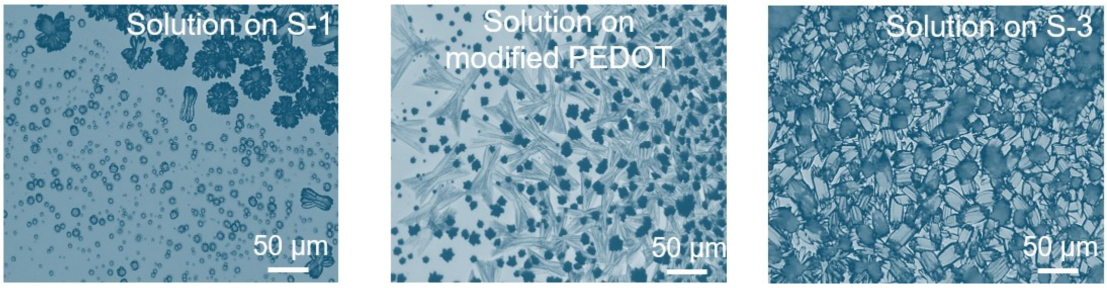

Figure S5. Optical images of Pb-Sn perovskite solution on modified PEDOT: PSS substrate, and S-1 and S-3 substrates are for comparation.

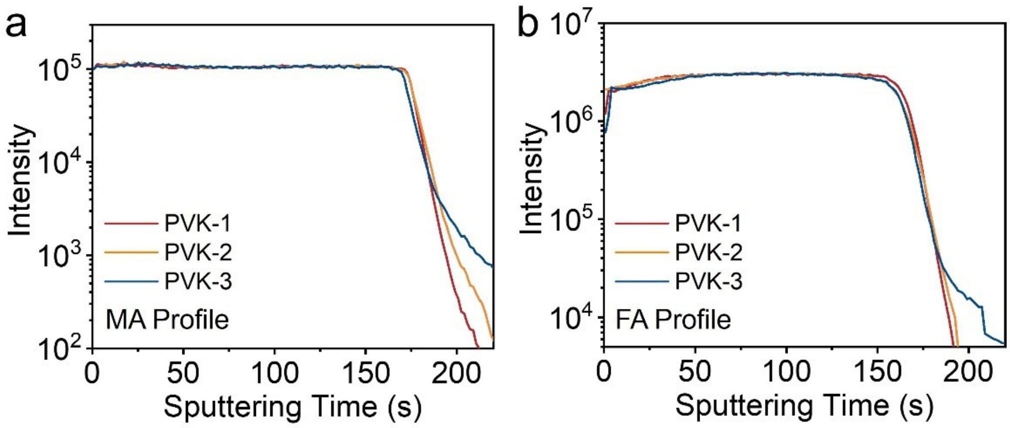

Figure S6. ToF-SIMS of (a) MA profile and (b) FA profile of the Pb-Sn films.

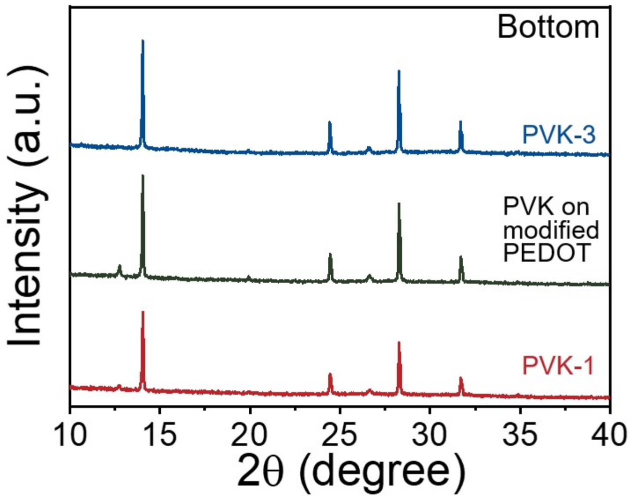

Figure S7. XRD patterns of bottom surface of PVK deposit on modified PEDOT: PSS, and PVK-1 and PVK-3 are for comparation.

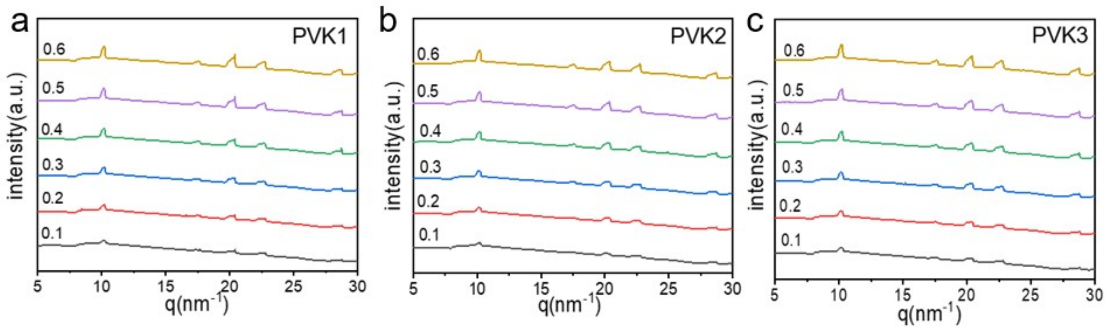

Figure S8. Depth-dependent GIWAXS profiles of the films with q from 5 – 30 nm^{-1}.

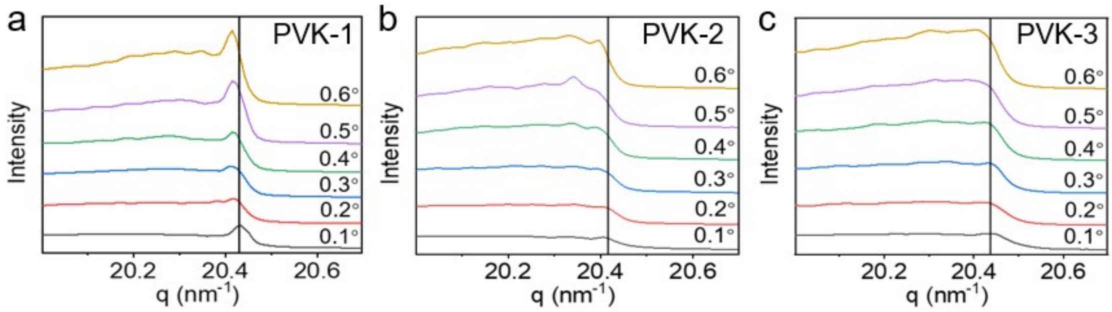

Figure S9. Zoom-in depth-dependent GIWAXS profiles of the films with q from 19.8 – 20.8 nm^{-1}.

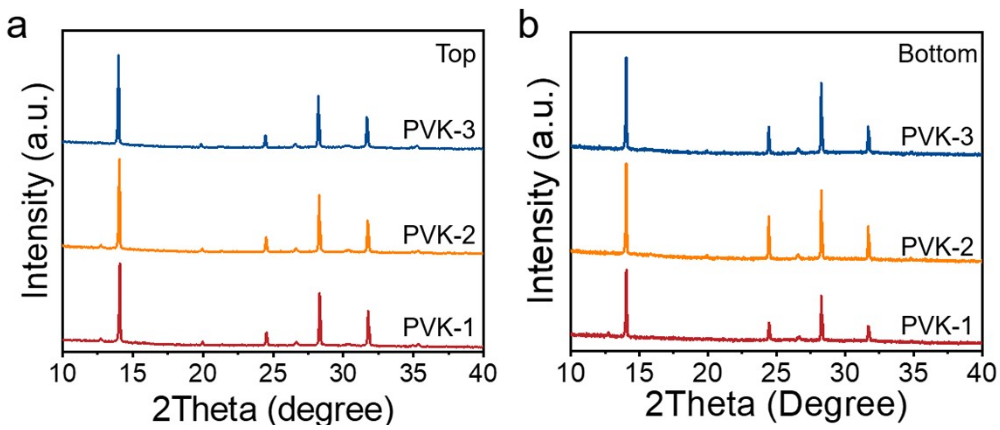

Figure S10. XRD patterns of top surface and bottom surfaces.

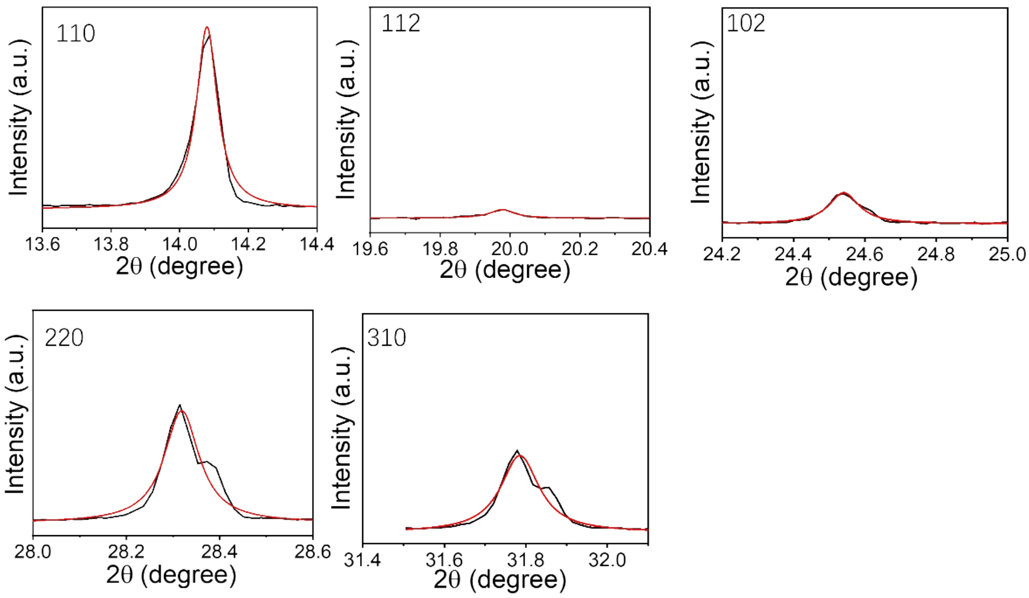

Figure S11. The peak fitting of the perovskite XRD on top of PVK1.

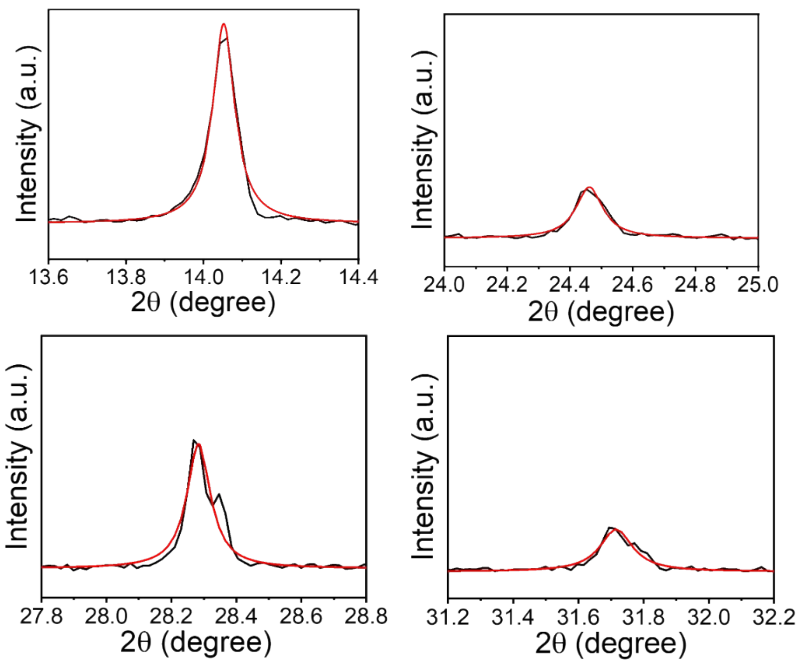

Figure S12.The peak fitting of the bottom XRD of PVK-1.

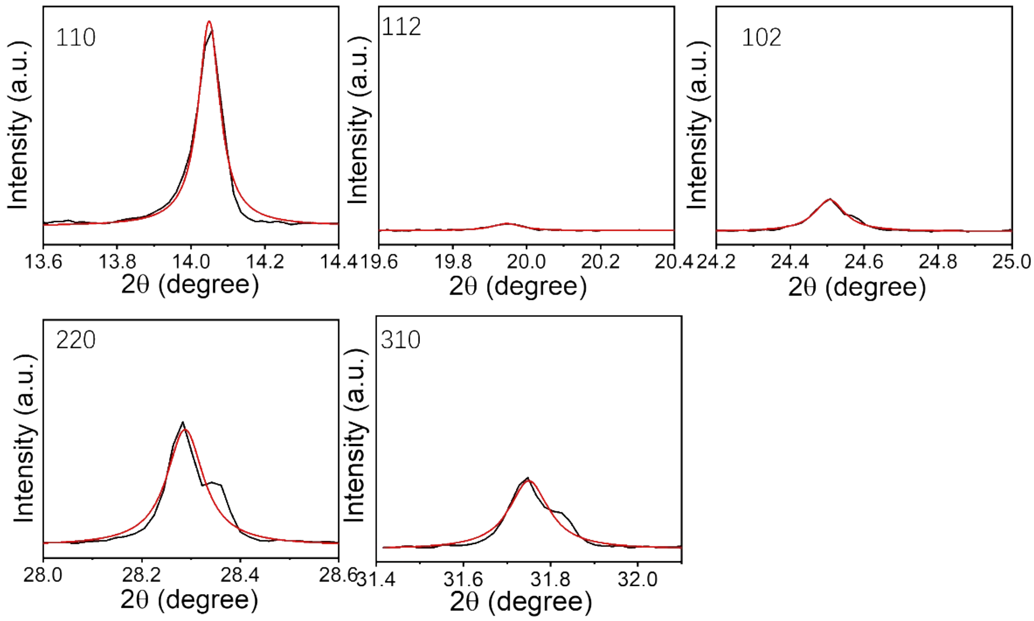

Figure S13. The peak fitting of the perovskite XRD on top of PVK2.

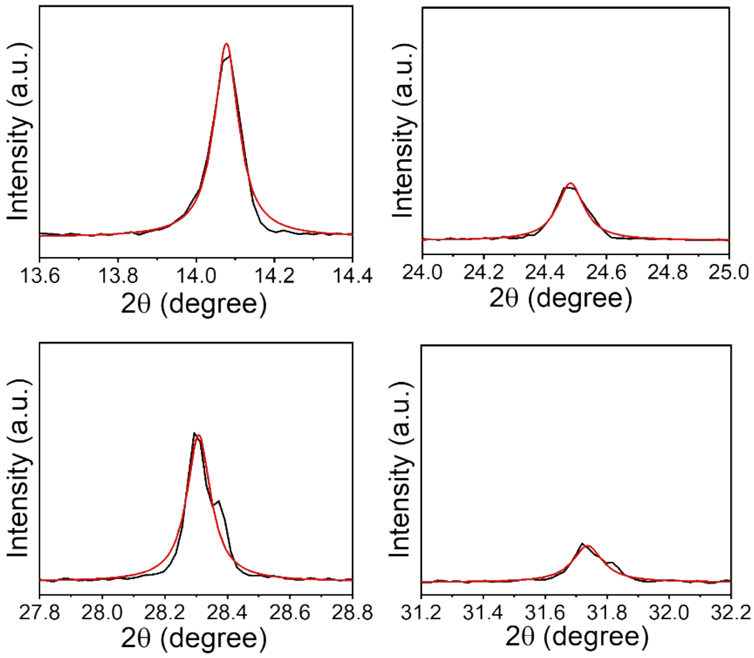

Figure S14.The peak fitting of the bottom XRD of PVK-2.

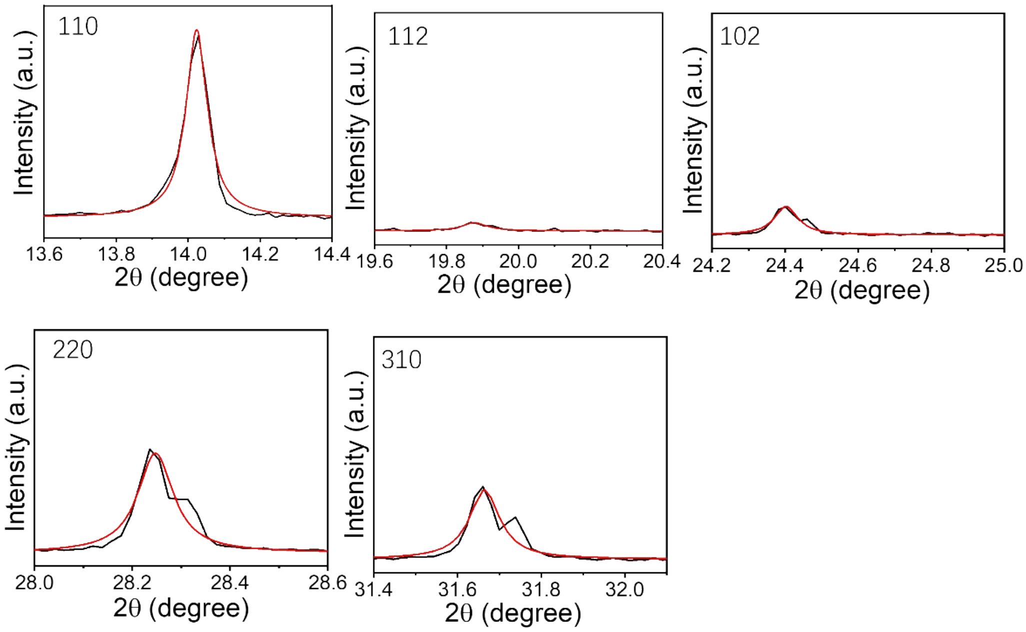

Figure S15. The peak fitting of the perovskite XRD on top of PVK3.

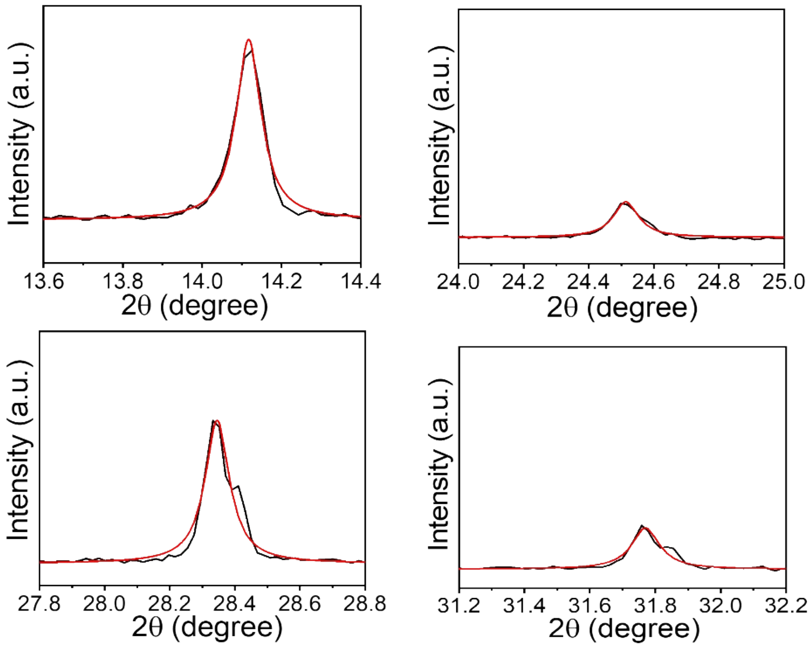

Figure S16. The peak fitting of the perovskite XRD on bottom of PVK3.

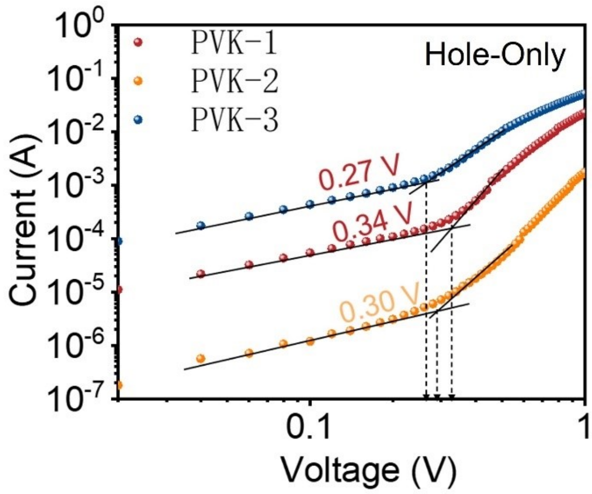

Figure S17. SCLC measurement of the hole-only devices based on different Pb-Sn films.

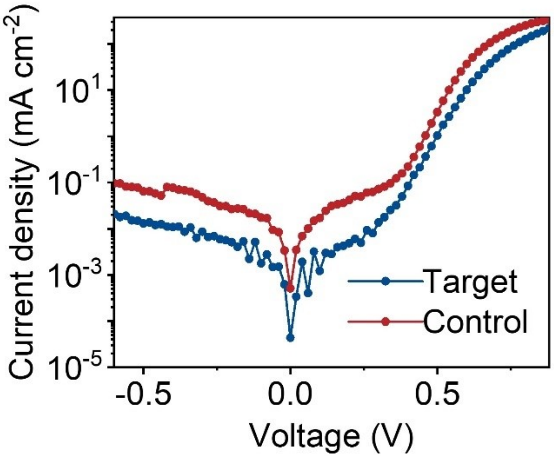

Figure S18. Dark current of control and target devices.

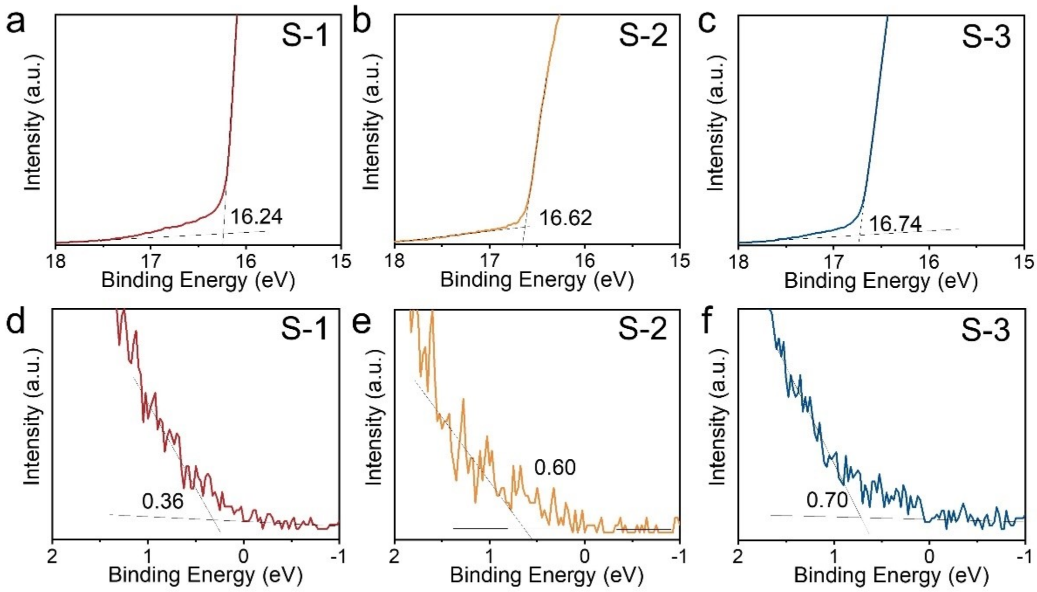

Figure S19. UPS of different substrates.

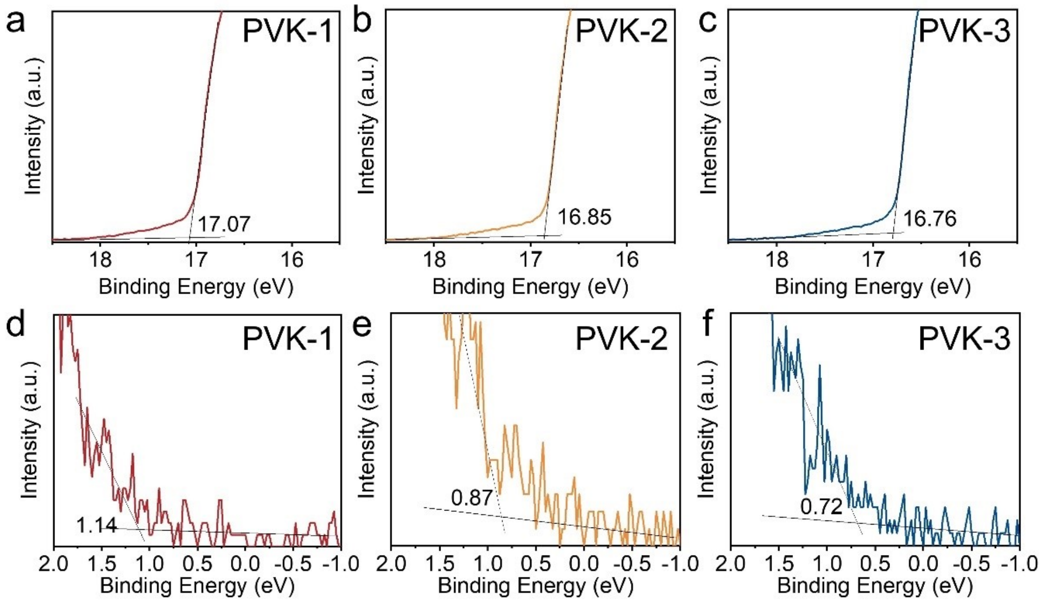

Figure S20. UPS of different Pb-Sn films.

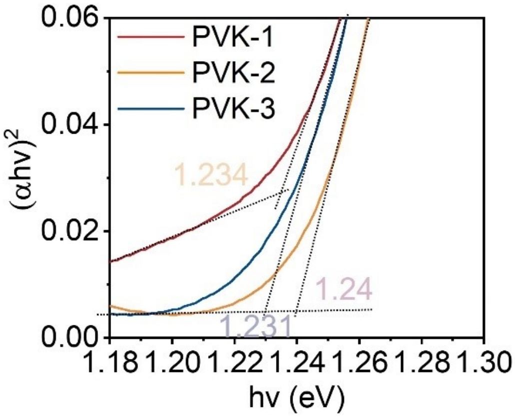

Figure S21. Tauc plots extracted from UV-Vis spectra of the Pb-Sn films.

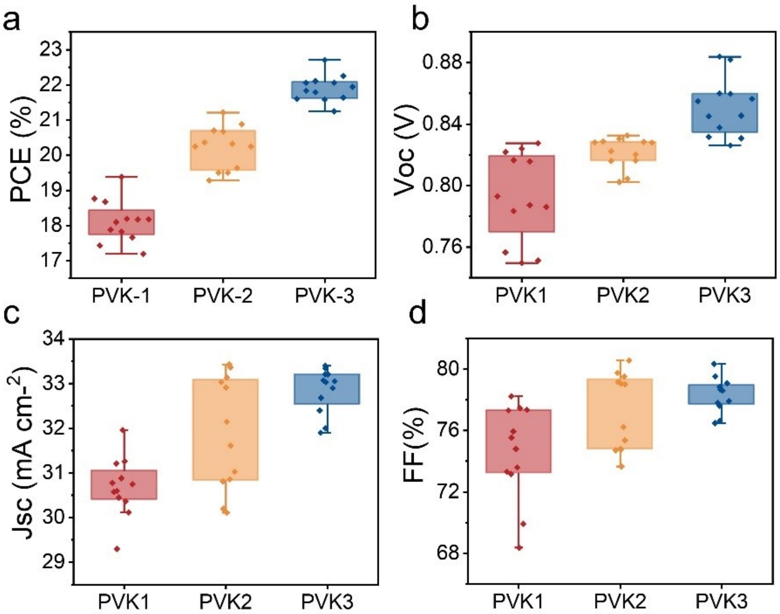

Figure S22. Statistics of (a) PCE, (b) V_{OC}, (c) J_{SC}, and (d) FF of the PSCs based on different Pb-Sn films.

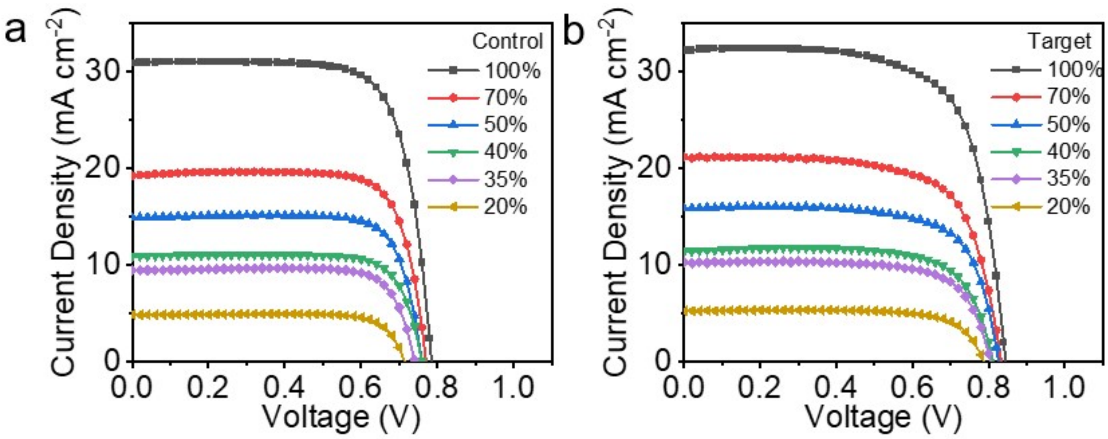

Figure S23. Light intensity dependent J-V curves of control and target device.

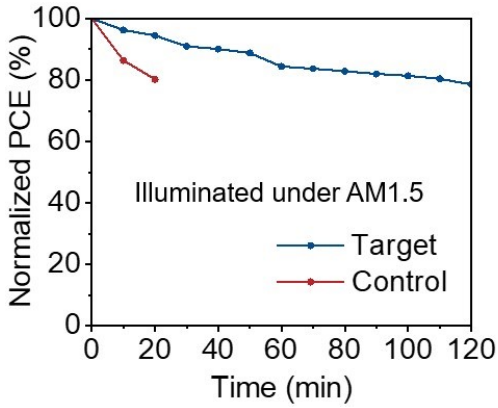

Figure S24. Light stability of unpackaged devices.

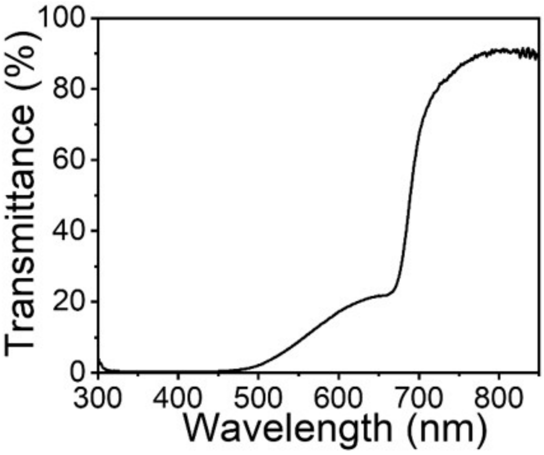

Figure S25. Transmission spectrum of the semi-transparent device used in this work.

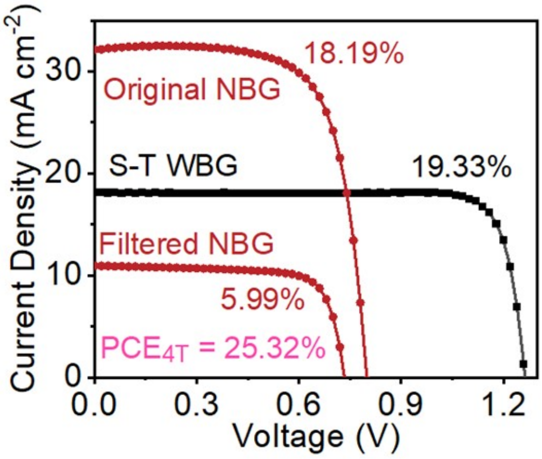

Figure S26. J-V curve of 4-T tandem device based on control Pb-Sn PSCs.

Table S1. The parameters of EIS.

Device	R_s (Ω)	R_{ct} (Ω)
PVK-1	10.38	3803
PVK-2	8.71	16071
PVK-3	7.545	23091

Table S2. Parameters calculated from SCLC of the films.

Film Label	Thickness (nm)	V_{TFL} (V)	N_{trap} ($cm^2V^{-1}S^{-1}$)
PVK-1	810	0.34	1.9×10^{15}
PVK-2	850	0.30	1.6×10^{15}
PVK-3	850	0.27	1.4×10^{15}

Table S3. Parameters of Control and Target devices in **Figure 6**c.

Device	Scan direction	V_{OC} (V)	J_{SC} (mA/cm^2)	FF (%)	PCE (%)	*HI* (%)
Control	Reverse	0.795	31.07	74.98	18.52	15.2
	Forward	0.790	29.66	67.05	15.71	
Target	Reverse	0.860	33.44	78.97	22.71	3.4
	Forward	0.853	33.34	77.08	21.92	

Table S4. Device parameters of the Target 4T tandem solar cell in this work.

Device	V_{OC} (V)	J_{SC} (mA cm^{-2})	FF (%)	PCE (%)
Pristine NBG	0.88	33.32	75.33	22.09
Semi-transparent WBG	1.27	18.11	84.04	19.33
Filtered NBG	0.85	12.39	79.29	8.35
4-Terminal Tandem	-	-	-	27.68

.

Table S5. A summary of recently reported Pb-Sn perovskite solar cells.

Year	Perovskite Composition	V_{OC} (V)	J_{SC} (mA/cm^{-2})	FF (%)	PCE (%)	Ref.
2023	$FA_{0.5}MA_{0.5}Sn_{0.5}Pb_{0.5}I_3$	0.88	31.0	78.4	21.4	[1]
2023	$FA_{0.7}MA_{0.3}Sn_{0.5}Pb_{0.5}I_3$	0.85	32.6	77.0	21.3	[2]
2023	$FA_{0.7}MA_{0.3}Sn_{0.5}Pb_{0.5}I_3$	0.81	30.6	80.9	20.00	[3]
2023	$FA_{0.7}MA_{0.3}Sn_{0.5}Pb_{0.5}I_3$	0.859	33.5	80.5	23.2	[4]
2023	$FA_{0.7}MA_{0.3}Sn_{0.5}Pb_{0.5}I_3$	0.85	32.31	80.26	22.07	[5]
2023	$FA_{0.5}MA_{0.5}Sn_{0.5}Pb_{0.5}I_3$	0.86	32.02	80.75	22.31	[6]
2023	$FA_{0.7}MA_{0.3}Sn_{0.5}Pb_{0.5}I_3$	0.78	27.79	75.05	16.44	[7]
2023	$FA_{0.7}MA_{0.3}Sn_{0.5}Pb_{0.5}I_3$	0.873	33.0	82.6	23.80	[8]
2023	$FA_{0.7}MA_{0.3}Sn_{0.5}Pb_{0.5}I_3$	0.84	30.94	78.99	20.35	[9]
2023	$FA_{0.7}MA_{0.3}Sn_{0.5}Pb_{0.5}I_3$	0.82	30.39	77.19	19.30	[10]
2023	$FA_{0.7}MA_{0.3}Sn_{0.5}Pb_{0.5}I_3$	0.89	31.69	79.90	22.46	[11]

2023	$FA_{0.7}MA_{0.3}Sn_{0.5}Pb_{0.5}I_3$	0.88	31.42	79.76	22.16	12
2023	$FA_{0.7}MA_{0.3}Sn_{0.5}Pb_{0.5}I_3$	0.87	31.98	77.97	21.57	13
2024	$FA_{0.7}MA_{0.3}Sn_{0.5}Pb_{0.5}I_3$	0.845	31.73	78.56	20.9	14
2024	$FA_{0.5}MA_{0.5}Sn_{0.5}Pb_{0.5}I_3$	0.89	32.51	77.12	22.31	15
Year	Perovskite Composition	V_{OC} (V)	J_{SC} (mA/cm^{-2})	FF (%)	PCE (%)	Ref.
2024	$FA_{0.7}MA_{0.3}Sn_{0.5}Pb_{0.5}I_3$	0.893	32.86	82.6	24.23	16
2024	$FA_{0.7}MA_{0.3}Sn_{0.5}Pb_{0.5}I_3$	0.853	32.88	80.0	22.44	17
2024	$FA_{0.7}MA_{0.3}Sn_{0.5}Pb_{0.5}I_3$	0.876	33.28	80.05	23.34	18
2024	$FA_{0.7}MA_{0.3}Sn_{0.5}Pb_{0.5}I_3$	0.853	29.34	80.08	20.03	19
2024	$FA_{0.7}MA_{0.3}Sn_{0.5}Pb_{0.5}I_3$	0.77	30.79	65.00	15.50	20
2024	$FA_{0.7}MA_{0.3}Sn_{0.5}Pb_{0.5}I_3$	0.84	32.63	73.49	20.14	21
2024	$FA_{0.7}MA_{0.3}Sn_{0.5}Pb_{0.5}I_3$	0.856	31.2	80.0	21.4	22
2024	$FA_{0.7}MA_{0.3}Sn_{0.5}Pb_{0.5}I_3$	0.88	32.99	78.46	22.79	23
2024	$FA_{0.5}MA_{0.5}Pb_{0.5}Sn_{0.5}I_3$	0.85	31.04	79.48	20.95	24
2024	$FA_{0.7}MA_{0.3}Sn_{0.5}Pb_{0.5}I_3$	0.87	32.68	81.59	23.24	25

2024	$FA_{0.7}MA_{0.3}Sn_{0.5}Pb_{0.5}I_3$	0.86	32.55	77.92	22.04	[26]
2025	$FA_{0.7}MA_{0.3}Sn_{0.5}Pb_{0.5}I_3$	0.87	33.52	78.56	22.71	**This work**

Table S6. A summary of the recently reported 4T all-perovskite tandem solar cells

Year	Bandgap of WBG/NBG (eV)	PCE of S-T WBG (%)	PCE of NBG (%)	PCE of Filtered NBG (%)	PCE of 4-T (%)	Ref.
2023	1.25/1.66	19.82	22.07	7.25	27.07	[5]
2023	1.78/1.25	18.25	21.83	9.80	28.05	[27]
2023	1.25/1.67	18.7	20.8	7.6	26.3	[28]
2023	1.25/1.77	17.68	21.57	9.99	27.67	[13]
2023	1.25/1.66	19.11	21.88	7.53	26.64	[29]
2024	1.25/1.66	20.13	21.24	7.93	28.06	[30]
2024	1.25/1.66	20.11	21.26	7.96	28.07	[31]
2024	1.25/1.77	18.41	21.66	10.05	28.46	[32]
2024	1.25/1.77	17.87	20.53	9.03	26.9	[33]

Year	Bandgap of WBG/NBG (eV)	PCE of S-T WBG (%)	PCE of NBG (%)	PCE of Filtered NBG (%)	PCE of 4-T (%)	Ref.
2024	1.24/1.66	19.17	22.10	7.72	26.89	34
2024	1.25/1.67	20.17	22.12	7.91	28.08	35
2024	1.25/1.77	17.61	20.72	8.48	26.09	36
2024	1.26/1.78	17.76	23.41	9.61	27.37	37
2024	1.25/1.78	18.36	21.20	9.95	28.31	26
2024	1.25/1.66	20.39	22.42	7.92	28.31	**38**
2024	1.25/1.67	20.06	22.75	8.29	28.35	39
2024	1.26/1.67	20.06	23.24	8.35	28.41	25
2024	1.27/1.78	19.12	21.79	8.01	27.13	40
2024	1.25/1.75	19.35	21.7	8.73	28.08	41
2025	1.25/1.77	19.11	23.54	9.1	28.22	42
2025	1.23/1.78	19.33	22.1	8.35	27.68	**This work**

References

1. Y. Xing, Z. Deng, T. Guo, Z. Zhang, Q. Tai, R. Zhao, J. Xiong, Q. Wang, L. Huang and X. Liu, *Chemical Engineering Journal*, 2023, **462**, 142122.
2. J. Song, T. Kong, Y. Zhang, X. Liu, M. Saliba and D. Bi, *Advanced Functional Materials*, 2023, **33**, 2304201.
3. K. Zhang, A. Vincze, E. Metwalli, J. Zhang, C. Liu, W. Meng, B. Zhang, J. Tian, T. Heumueller and Z. Xie, *Advanced Functional Materials*, 2023, **33**, 2303455.
4. C. Liu, R. Lin, Y. Wang, H. Gao, P. Wu, H. Luo, X. Zheng, B. Tang, Z. Huang and H. Sun, *Angewandte Chemie*, 2023, **135**, e202313374.
5. W. Zhang, L. Huang, H. Guan, W. Zheng, Z. Li, H. Cui, S. Zhou, J. Liang, G. Li and T. Wang, *Energy & Environmental Science*, 2023, **16**, 5852-5862.
6. R. Meng, C. Li, J. Shi, Z. Wan, Z. Li, C. Zhi, Y. Zhang and Z. Li, *ACS Energy Letters*, 2023, **8**, 5206-5214.
7. Y. Li, S. Yan, J. Cao, H. Chen, B. Liu, J. Xie, Y. Shu, F. Wang, A. Wang and J. Dong, *npj Flexible Electronics*, 2023, **7**, 18.
8. R. Lin, Y. Wang, Q. Lu, B. Tang, J. Li, H. Gao, Y. Gao, H. Li, C. Ding and J. Wen, *Nature*, 2023, **620**, 994-1000.
9. W. Chen, Y. Huang, H. Cui, S. Li, Y. Feng and B. Zhang, *Small Methods*, 2023, **7**, 2201276.

10. Y. Liu, W. Gao, G. Xing, S. Lv, X. Zhao, J. Yang, L. Chao, Z. Wu, Y. Xia and C. Ran, *Solar RRL*, 2023, **7**, 2300575.
11. S. Zhou, S. Fu, C. Wang, W. Meng, J. Zhou, Y. Zou, Q. Lin, L. Huang, W. Zhang, G. Zeng, D. Pu, H. Guan, C. Wang, K. Dong, H. Cui, S. Wang, T. Wang, G. Fang and W. Ke, *Nature*, 2023, **624**, 69-73.
12. L. Huang, H. Cui, W. Zhang, D. Pu, G. Zeng, Y. Liu, S. Zhou, C. Wang, J. Zhou, C. Wang, H. Guan, W. Shen, G. Li, T. Wang, W. Zheng, G. Fang and W. Ke, *Advanced Materials*, 2023, **35**, 2301125.
13. W. Chen, H. Guan, L. Huang, J. Zhou, S. Zhou, D. Pu, G. Zeng, C. Wang, Y. Ge, C. Wang, W. Shen, H. Fang, G. Li, Q. Lin, G. Fang, W. Ke and Q. Liu, *Solar RRL*, 2024, **8**, 2300896.
14. Z. Xie, S. Chen, Y. Pei, L. Li, S. Zhang and P. Wu, *Chemical Engineering Journal*, 2024, **482**, 148638.
15. B. Liu, H. Chen, J. Cao, X. Chen, J. Xie, Y. Shu, F. Yan, W. Huang and T. Qin, *Advanced Functional Materials*, 2024, **34**, 2310828.
16. J. Song, T. Kong, Z. Zhao, Y. Zhang, Y. Liu and D. Bi, *Advanced Functional Materials*, 2024, 2411746.
17. G. Chen, G. Su, X. Zhang, Q. Sun, H. Gao, K. Liu, H. Li, J. Wang, D. He and G. Ma, *Nano Energy*, 2024, **131**, 110248.
18. H. Liu, C. Li, J. Dong, Y. Dai, P. Wang, B. Shi, Y. Zhao and X. Zhang, *Advanced Energy Materials*, 2024, **14**, 2304234.
19. S. Siegrist, J. Kurisinkal Pious, H. Lai, R. K. Kothandaraman, J. Luo, V. Vlnieska, A. N. Tiwari and F. Fu, *Solar RRL*, 2024, **8**, 2400447.
20. T. Song, H. Jang, J. Seo, J. Roe, S. Song, J. W. Kim, J. Yeop, Y. Lee, H. Lee and S. Cho, *ACS nano*, 2024, **18**, 2992-3001.
21. T. Zhang, F. Qian, Y. Zhai, J. Li, L. Wang, Z. Diao, S. Yuan, H. Zheng, Y. Wang and Y. Gong, *ACS Applied Materials & Interfaces*, 2024, **16**, 13763-13772.
22. H. Gao, K. Xiao, R. Lin, S. Zhao, W. Wang, S. Dayneko, C. Duan, C. Ji, H. Sun and A. D. Bui, *Science*, 2024, **383**, 855-859.
23. J. Zhou, S. Fu, S. Zhou, L. Huang, C. Wang, H. Guan, D. Pu, H. Cui, C. Wang,

T. Wang, W. Meng, G. Fang and W. Ke, *Nature Communications*, 2024, **15**, 2324.

24. W. Shen, H. Fang, D. Pu, W. Zheng, X. Zhang, G. Li, L. Huang, S. Zhou, W. Chen, Y. Zhou, Z. Feng, J. Liang, J. Zhou, P. Qin, G. Fang and W. Ke, *Advanced Functional Materials*, 2024, **34**, 2410605.
25. G. Li, C. Wang, S. Fu, W. Zheng, W. Shen, P. Jia, L. Huang, S. Zhou, J. Zhou, C. Wang, H. Guan, Y. Zhou, X. Zhang, D. Pu, H. Fang, Q. Lin, W. Ai, W. Chen, G. Zeng, T. Wang, P. Qin, G. Fang and W. Ke, *Advanced Materials*, 2024, **36**, 2401698.
26. G. Zeng, W. Chen, H. Guan, W. Meng, H. Cui, S. Zhou, L. Huang, D. Pu, H. Fang, H. Liu, S. Hou, T. Yu, G. Fang and W. Ke, *Advanced Functional Materials*, **n/a**, 2412458.
27. H. Cui, L. Huang, S. Zhou, C. Wang, X. Hu, H. Guan, S. Wang, W. Shao, D. Pu, K. Dong, J. Zhou, P. Jia, W. Wang, C. Tao, W. Ke and G. Fang, *Energy & Environmental Science*, 2023, **16**, 5992-6002.
28. X. Hu, J. Li, C. Wang, H. Cui, Y. Liu, S. Zhou, H. Guan, W. Ke, C. Tao and G. Fang, *Nano-Micro Letters*, 2023, **15**, 103.
29. H. Guan, W. Zhang, J. Liang, C. Wang, X. Hu, D. Pu, L. Huang, Y. Ge, H. Cui, Y. Zou, G. Fang and W. Ke, *Advanced Functional Materials*, 2023, **33**, 2300860.
30. H. Guan, S. Zhou, S. Fu, D. Pu, X. Chen, Y. Ge, S. Wang, C. Wang, H. Cui and J. Liang, *Advanced Materials*, 2024, **36**, 2307987.
31. X. Hu, F. Yao, C. Wang, H. Cui, P. Jia, S. Du, S. Zhou, H. Guan, Q. Lin, W. Ke, C. Tao and G. Fang, *Chemical Engineering Journal*, 2024, **489**, 151379.
32. H. Guan, S. Fu, G. Zeng, W. Chen, C. Wang, H. Cui, D. Pu, P. Jia, W. Meng, G. Fang and W. Ke, *Energy & Environmental Science*, 2024, **17**, 8219-8227.
33. Z. Yi, W. Wang, R. He, J. Zhu, W. Jiao, Y. Luo, Y. Xu, Y. Wang, Z. Zeng and K. Wei, *Energy & Environmental Science*, 2024, **17**, 202-209.
34. Y. Dong, R. Yu, G. Su, Z. Ma, Z. He, R. Wang, Y. Zhang, J. Yang, Y. Gong and M. Li, *Advanced Materials*, 2024, 2312704.

35. Y. Guo, S. Du, X. Hu, G. Li, Z. Yu, H. Guan, S. Wang, P. Jia, H. Zhou and C. Li, *Nano Energy*, 2024, **126**, 109612.
36. X. Lian, Y. Xu, W. Fu, R. Meng, Q. Ma, C. Xu, M. Luo, Y. Hu, J. Han and H. Min, *Advanced Functional Materials*, 2024, 2402061.
37. J. Xie, X. Jin, J. Cao, Y. Shu, W. Yan, L. Han, J. Duan, F. Wang, J. Dong and A. Wang, *Advanced Functional Materials*, 2024, 2414819.
38. S. Du, Y. Guo, C. Wang, G. Chen, G. Li, J. Liang, W. Chen, Z. Yu, Y. Ge and P. Jia, *Advanced Energy Materials*, 2404180.
39. P. Jia, G. Chen, G. Li, J. Liang, H. Guan, C. Wang, D. Pu, Y. Ge, X. Hu and H. Cui, *Advanced Materials*, 2024, 2400105.
40. G. Xing, C. Li, W. Gao, J. Yang, X. Zhao, J. Wang, X. Ran, L. Chao, H. Huang and Y. Zhou, *Advanced Materials*, 2024, **36**, 2404185.
41. R. Wang, X. Liu, S. Yan, N. Meng, X. Zhao, Y. Chen, H. Li, S. M. H. Qaid, S. Yang, M. Yuan and T. He, *Nature Communications*, 2024, **15**, 8899.
42. J. Zhu, X. Huang, Y. Luo, W. Jiao, Y. Xu, J. Wang, Z. Gao, K. Wei, T. Ma, J. You, J. Jin, S. Wu, Z. Zhang, W. Liang, Y. Wang, S. Ren, C. Wang, C. Chen, J. Zhang and D. Zhao, *Nature Communications*, 2025, **16**, 240.